Synthesis and Characterization of NiSn Dendrimer-Encapsulated Nanoparticles

Arther T. Gates, Elizabeth G. Nettleton, V. Sue Myers, and Richard M. Crooks*

Department of Chemistry and Biochemistry and the Center for Electrochemistry, The University of Texas at Austin, 1 University Station A5300, Austin, Texas 78712-0165

We report the synthesis and characterization of NiSn dendrimer-encapsulated nanoparticles (DENs) with sizes in the range of ~1.2 nm. These types of materials have potential applications in energy storage, and particles in the 1−3 nm size range are particularly attractive for this use. The NiSn DENs described here contain an average of 147 atoms and are encapsulated within hydrophobic, sixth-generation poly(amidoamine) dendrimers. DENs prepared using four different Ni/Sn ratios, along with monometallic Ni and Sn DENs, are described. To prevent oxidation, the synthesis was carried out under dry conditions in toluene. These bimetallic DENs were characterized by UV−vis spectroscopy, transmission electron microscopy, energy-dispersive X-ray spectroscopy, and X-ray photoelectron spectroscopy. The results indicate that the compositions of the nanoparticles reflect the ratio of Ni^{2+} and Sn^{2+} used in the first step of the synthesis; the NiSn nanoparticles remain encapsulated within the dendrimers, and when dry they have a degree of stability even after a short exposure to air.

Introduction

We report the synthesis and characterization of dendrimer-encapsulated nanoparticles (DENs)[1] consisting of an average of 147 atoms and containing specific Ni/Sn ratios. The findings reported here are significant for two reasons. First, DENs composed of two easily oxidized metals have not previously been reported. Second, NiSn nanoparticles having diameters of 1−3 nm are relevant to Li ion battery technology but are not attainable using conventional synthesis strategies. Transmission electron microscopy (TEM) indicates that the NiSn DENs reported here have diameters of ~1.2 nm, and energy-dispersive X-ray (EDX) spectroscopy establishes their bimetallic composition.

The dendrimer templating method provides a straightforward and versatile means of preparing nanoparticles having diameters of < 3 nm in either aqueous or organic solvents.[1] The dendrimer template synthesis is usually performed in two steps. First, metal ions are mixed with the dendrimers, which results in sequestration of the ions within the interior of the dendrimer template. Second, the metal ion/dendrimer complex is chemically reduced to yield encapsulated nanoparticles. We have reported previously that the size of DENs is determined by the metal ion/dendrimer ratio used to form the complex[2] and that the chemical composition of bimetallic DENs is defined by the relative number of different metal ions used in their preparation.[3] The zerovalent nanoparticles that result from this synthesis are sequestered inside the dendrimers and thus stabilized against agglomeration. However, small molecules are able to penetrate the dendrimer and access the encapsulated nanoparticle; therefore, DENs are useful for applications related to energy storage and catalysis.[4,5]

DENs are normally synthesized in water using either NH₂- or OH-terminated poly(amidoamine) (PAMAM) dendrimer templates. This approach has been used by us and others to prepare Au,[6−10] Pt,[11−18] Pd,[19−24] Cu,[25] AuAg,[26,27] PtPd,[3,28−31] PtCu,[32,33]

*To whom correspondence should be addressed. E-mail: crooks@cm.utexas.edu. Phone: 512-475-8674.

(1) Scott, R. W. J.; Wilson, O. M.; Crooks, R. M. *J. Phys. Chem. B* **2005**, *109*, 692–704.
(2) Ye, H.; Crooks, J. A.; Crooks, R. M. *Langmuir* **2007**, *23*, 11901–11906.
(3) Ye, H.; Crooks, R. M. *J. Am. Chem. Soc.* **2007**, *129*, 3627–3633.
(4) Niu, Y.; Crooks, R. M. *C. R. Chim.* **2003**, *6*, 1049–1059.
(5) Crump, C. J.; Gilbertson, J. D.; Chandler, B. D. *Top. Catal.* **2008**, *49*, 233–240.
(6) Tran, M. L.; Zvyagin, A. V.; Plakhotnik, T. *Chem. Commun.* **2006**, 2400–2401.
(7) Groehn, F.; Bauer, B. J.; Akpalu, Y. A.; Jackson, C. L.; Amis, E. J. *Macromolecules* **2000**, *33*, 6042–6050.
(8) Groehn, F.; Gu, X.; Gruell, H.; Meredith, J. C.; Nisato, G.; Bauer, B. J.; Karim, A.; Amis, E. J. *Macromolecules* **2002**, *35*, 4852–4854.
(9) Esumi, K.; Satoh, K.; Torigoe, K. *Langmuir* **2001**, *17*, 6860–6864.
(10) Kim, Y.-G.; Oh, S.-K.; Crooks, R. M. *Chem. Mater.* **2004**, *16*, 167–172.
(11) Alexeev, O. S.; Siani, A.; Lafaye, G.; Williams, C. T.; Ploehn, H. J.; Amiridis, M. D. *J. Phys. Chem. B* **2006**, *110*, 24903–24914.
(12) Esumi, K.; Nakamura, R.; Suzuki, A.; Torigoe, K. *Langmuir* **2000**, *16*, 7842–7846.
(13) Lang, H.; May, R. A.; Iversen, B. L.; Chandler, B. D. *J. Am. Chem. Soc.* **2003**, *125*, 14832–14836.
(14) Oh, S.-K.; Kim, Y.-G.; Ye, H.; Crooks, R. M. *Langmuir* **2003**, *19*, 10420–10425.
(15) Vijayaraghavan, G.; Stevenson, K. J. *Langmuir* **2007**, *23*, 5279–5282.
(16) Ye, H.; Crooks, R. M. *J. Am. Chem. Soc.* **2005**, *127*, 4930–4934.
(17) Ye, H.; Scott, R. W. J.; Crooks, R. M. *Langmuir* **2004**, *20*, 2915–2920.
(18) Zhao, M.; Crooks, R. M. *Adv. Mater.* **1999**, *11*, 217–220.
(19) Chechik, V.; Crooks, R. M. *J. Am. Chem. Soc.* **2000**, *122*, 1243–1244.
(20) Garcia-Martinez, J. C.; Lezutekong, R.; Crooks, R. M. *J. Am. Chem. Soc.* **2005**, *127*, 5097–5103.
(21) Niu, Y.; Crooks, R. M. *Chem. Mater.* **2003**, *15*, 3463–3467.
(22) Ooe, M.; Murata, M.; Mizugaki, T.; Ebitani, K.; Kaneda, K. *Nano Lett.* **2002**, *2*, 999–1002.
(23) Wilson, O. M.; Knecht, M. R.; Garcia-Martinez, J. C.; Crooks, R. M. *J. Am. Chem. Soc.* **2006**, *128*, 4510–4511.
(24) Yeung, L. K.; Crooks, R. M. *Nano Lett.* **2001**, *1*, 14–17.
(25) Zhao, M.; Sun, L.; Crooks, R. M. *J. Am. Chem. Soc.* **1998**, *120*, 4877–4878.
(26) Garcia-Martinez, J. C.; Wilson, O. M.; Scott, R. W. J.; Crooks, R. M. *ACS Symp. Ser.* **2006**, *928*, 215−229.
(27) Wilson, O. M.; Scott, R. W. J.; Garcia-Martinez, J. C.; Crooks, R. M. *J. Am. Chem. Soc.* **2005**, *127*, 1015–1024.
(28) Peng, X. H.; Pan, Q. M.; Rempel, G. L.; Wu, S. *Catal. Commun.* **2009**, *11*, 62–66.
(29) Scott, R. W. J.; Datye, A. K.; Crooks, R. M. *J. Am. Chem. Soc.* **2003**, *125*, 3708–3709.
(30) Ye, H.; Crooks, R. M. *Polym. Prepr. (Am. Chem. Soc., Div. Polym. Chem.)* **2006**, *47*, 845–846.
(31) Chung, Y.-M.; Rhee, H.-K. *Catal. Lett.* **2003**, *85*, 159–164.
(32) Hoover, N. N.; Auten, B. J.; Chandler, B. D. *J. Phys. Chem. B* **2006**, *110*, 8606–8612.
(33) Myers, S. V.; Frenkel, A. I.; Crooks, R. M. *Chem. Mater.* **2009**, *21*, 4824–4829.
(34) Knecht, M. R.; Weir, M. G.; Frenkel, A. I.; Crooks, R. M. *Chem. Mater.* **2008**, *20*, 1019–1028.

PdAu,[34−38] and PdRh DENs.[28] We have also shown that Au DENs[39] and monometallic DENs of easily oxidized metals, such as Cu,[21] Ni,[40] and Fe,[41] can be synthesized in organic solvents using hydrophobic dendrimers. However, the synthesis and characterization of bimetallic DENs consisting of two reactive metals have not previously been reported.

The ongoing effort to advance Li ion battery technology has created a demand for new high-energy-density anode materials capable of withstanding the physical stress incurred during charge/discharge cycles. In this regard, bimetallic materials containing Sn show promise as alternatives to traditional graphite-based electrodes. For example, Ni_3Sn_4 phases provide a nearly 3-fold enhancement in theoretical capacity (993 mA h/g of Sn) compared to that of graphite anodes.[42−44] However, micrometer-sized NiSn anode materials have limited performance lifetimes (∼40 cycles),[45] which are caused by volume fluctuations associated with the ingress and egress of Li^+. In contrast, nanoscale NiSn anodes are better able to accommodate size changes; therefore, they have been shown to have extended cycle lives (>200 cycles).[46]

Electrodeposition and solvothermal methods are typically used to prepare nanoscale NiSn anode materials. For example, electrodeposition has been used to decorate the surfaces of vertically arrayed 200-nm-diameter Cu nanorods with 50 nm Ni_3Sn_4 nanoparticles.[46] Nanoscale NiSn anodes have also been fabricated using chemical liquid deposition, which yields NiSn nanoparticles having an average diameter of ∼6 nm but with a relatively high polydispersity (3−10 nm).[47,48] The solvothermal approach has also been used to prepare even larger Ni_3Sn_2 anode phases of ∼30 nm.[49] The synthesis of well-defined NiSn nanoparticles having dimensions of <3 nm has not been reported.

Here we describe the synthesis and characterization of well-defined bimetallic NiSn DENs having diameters of ∼1.2 nm. These materials are prepared within hydrophobic PAMAM dendrimers functionalized on their periphery with dodecyl groups. The synthesis is carried out in toluene, and it involves the sequestration of both Ni^{2+} and Sn^{2+} within the interior voids of the dendrimers. We have not observed spectral signatures of specific interactions between the metal ions and dendrimer functional groups, and thus it seems likely that encapsulation is driven by the enhanced solubility of the metal ions in the relatively high dielectric interior of the dendrimers.[39] Reduction of the metal ion/dendrimer complex with triethylborohydride leads to zerovalent, bimetallic NiSn DENs. The elemental composition of these DENs is determined by the

(35) Scott, R. W. J.; Sivadinarayana, C.; Wilson, O. M.; Yan, Z.; Goodman, D. W.; Crooks, R. M. *J. Am. Chem. Soc*. **2005**, *127*, 1380–1381.
(36) Scott, R. W. J.; Wilson, O. M.; Crooks, R. M. *Chem. Mater*. **2004**, *16*, 5682–5688.
(37) Scott, R. W. J.; Wilson, O. M.; Oh, S.-K.; Kenik, E. A.; Crooks, R. M. *J. Am. Chem. Soc*. **2004**, *126*, 15583–15591.
(38) Weir, M. G.; Knecht, M. R.; Frenkel, A. I.; Crooks, R. M. *Langmuir* **2010**, *26*, 1137–1146.
(39) Knecht, M. R.; Garcia-Martinez, J. C.; Crooks, R. M. *Langmuir* **2005**, *21*, 11981–11986.
(40) Knecht, M. R.; Garcia-Martinez, J. C.; Crooks, R. M. *Chem. Mater*. **2006**, *18*, 5039–5044.
(41) Knecht, M. R.; Crooks, R. M. *New J. Chem*. **2007**, *31*, 1349–1353.
(42) Bruce, P. G.; Scrosati, B.; Tarascon, J.-M. *Angew. Chem., Int. Ed*. **2008**, *47*, 2930–2946.
(43) Kim, M. G.; Cho, J. *Adv. Funct. Mater*. **2009**, *19*, 1497–1514.
(44) Palacin, M. R. *Chem. Soc. Rev*. **2009**, *38*, 2565–2575.
(45) Hassoun, J.; Panero, S.; Scrosati, B. *Adv. Mater*. **2006**, *160*, 1336–1341.
(46) Hassoun, J.; Panero, S.; Simon, P.; Taberna, P. L.; Scrosati, B. *Adv. Mater*. **2007**, *19*, 1632–1635.
(47) Cardenas, G.; Leon, Y. *Colloid Polym. Sci*. **2003**, *282*, 394–481.
(48) Cardenas, G.; Leon, Y.; Pena, O. *Colloid Polym. Sci*. **2006**, *284*, 644–653.
(49) Qin, H.; Zhao, X.; Jiang, N.; Li, Z. *J. Power Sources* **2007**, *171*, 948–952.

stoichometric ratio of Ni^{2+} to Sn^{2+} used to form the dendrimer complex.

Experimental Section

Chemicals. Sixth-generation, dodecyl-terminated PAMAM dendrimers (G6-C_{12}) in methanol were purchased from Dendritech, Inc. (Midland, MI). The dendrimer solution was dried under vacuum to remove methanol, and the resulting residue was reconstituted in sufficient toluene to yield a 200 μM stock solution. Nickel perchlorate ($Ni(ClO_4)_2 \cdot 6H_2O$), tin triflate (Sn-$(CF_3SO_3)_2$), 1.0 M sodium triethylborohydride ($Na(C_2H_5)_3BH$) in toluene, and anhydrous solvents (toluene and tetrahydrofuran (THF)) were purchased from Sigma-Aldrich. ***Caution! Ni-$(ClO_4)_2 \cdot 6H_2O$ is a strong oxidizing agent and should be handled with extreme care.*** Stock solutions of the metal salts (10.0 mM) were prepared in THF. All reagents and stock solutions were prepared and kept in a N_2-purged glovebox to avoid exposure to the atmosphere.

Synthesis of DENs. DENs were synthesized via the co-complexation method[1] under N_2 atmosphere to prevent oxidation of the product. A total of six different DEN compositions, each containing an average of 147 metal atoms, were prepared. These are denoted as G6-$C_{12}(Ni_xSn_{(147−x)})$ (x = 147, 110, 73.5, 63.0, 37.0, and 0). Here, the subscripts reflect only the Ni/dendrimer and Sn/dendrimer ratios used in the synthesis; they are not intended to reflect the exact compositions of individual complexes or DENs. We chose DENs containing an average of 147 atoms for three reasons. First, this is the number of atoms in a closed-shell cuboctahedron. However, we do not wish to imply any specific knowledge of the structure of these Ni/Sn DENs. Second, 147 is intermediate between the smallest (∼40 atoms) and largest (∼240 atoms) DENs that are possible to prepare in G6 PAMAM dendrimers. Third, we have previously reported numerous other metallic and bimetallic DENs having 147 atoms, so for consistency we chose that value for the current study.

For a typical synthesis, 50.0 μL of the G6-C_{12} stock solution was added to toluene with stirring to yield a concentration of 2.00 μM. Requisite volumes of 10.0 mM $Ni(ClO_4)_2 \cdot 6H_2O$ and/or $Sn(CF_3SO_3)_2$ stock solution (in THF) were then added to the dendrimer solution to achieve the desired Ni^{2+}/Sn^{2+} stoichiometry. This solution was stirred for 1 h to provide sufficient time for encapsulation of the metal ions. Reduction of the complex was initiated by the addition of 50 μL of 1 M $Na(C_2H_5)_3BH$. The latter solution was stirred for at least 1 h prior to characterization.

Characterization. UV−vis absorption spectra of the DEN solutions were acquired with a Hewlett-Packard HP8453 spectrometer using 1.00-cm-path-length quartz cuvettes that were sealed under N_2 prior to spectral analysis. Background subtraction was achieved with a blank solution containing 2.00 μM G6-C_{12} in toluene. TEM imaging and elemental analysis were performed using an FEI TECNAI G2 F20 X-TWIN electron microscope (200 kV acceleration voltage) equipped with an EDX detector. Samples for TEM studies were prepared in a N_2 glovebox by dropping 5.00 μL of the DEN solution onto carbon-coated Au grids (400 mesh) and drying. X-ray photoelectron spectroscopy (XPS) studies were carried out using a Kratos Axis Ultra spectrometer equipped with Al Kα and Mg Kα radiation sources. Spectra were collected at a pass energy of 20 eV and a step size of 0.5 eV.

Results and Discussion

Synthesis and UV−Vis Analysis of G6-$C_{12}(Ni_xSn_{(147−x)})$ DENs. Nanoparticles composed of reactive metals such as Ni and Sn typically degrade in the presence of O_2 or H_2O. Accordingly, the NiSn DENs described here were synthesized under dry, O_2-free conditions.[40] The synthesis was carried out in two steps. First, an appropriate Ni^{2+}/Sn^{2+} ratio (in THF) was added to a toluene solution containing hydrophobic G6-C_{12} dendrimers.

This results in the formation of a fully soluble metal ion/dendrimer complex. Second, a 10-fold molar excess of the triethylborohydride reducing agent was added to the complex solution to yield the bimetallic DENs. More details regarding the synthesis are provided in the Experimental Section.

Figure 1 shows representative UV−vis absorption spectra for solutions containing the G6-C$_{12}$(Ni$_x$Sn$_{(147−x)}$) (x = 147, 110, 73.5, 63.0, 37.0, and 0) precursor complex before and after reduction. The complexes (prior to reduction) were fully soluble, but their spectra (Figure 1a) are featureless. In contrast, when the Ni^{2+} and Sn^{2+} salts are added to toluene in the absence of the dendrimer, precipitation occurs immediately. We conclude that solubility differences between the dendrimer interior and the toluene phase drive the metal salts into the dendrimer.[39]

After reduction, the solution of G6-C$_{12}$(Ni$_{147}$) DENs appears dark brown in color, and the spectrum in Figure 1b exhibits a broad monotonically decreasing absorption band. This result is consistent with previous observations for G6-C$_{12}$(Ni$_{147}$) DENs.[40] In contrast, monometallic Sn DENs yielded a significantly lower absorbance and appeared just slightly golden in color. The spectral properties observed for Sn DENs in toluene are consistent with theoretical predictions for nanoscale Sn colloids dispersed in a low-dielectric solvent.[50] The absorbances of bimetallic NiSn DENs were intermediate between those of the monometallic Ni and Sn materials and increased roughly proportionately with Ni content. All of the G6-C$_{12}$(Ni$_x$Sn$_{(147−x)}$) DENs are stable in a N$_2$ atmosphere, but they quickly precipitate upon exposure to air.[40]

TEM Analysis of NiSn DENs. Figure 2a is a representative TEM micrograph of G6-C$_{12}$(Sn$_{147}$) DENs, and it indicates the formation of distinct nanoparticles. Figure 2b is the corresponding size distribution histogram, showing that the average diameter of the monometallic G6-C$_{12}$(Sn$_{147}$) DENs is 1.9 ± 0.3 nm. This value can be compared to a diameter of 1.96 calculated for 147-atom Sn nanoparticles using the assumptions given in the footnote in Table 1. Figure 2c is a TEM micrograph of the bimetallic G6-C$_{12}$(Ni$_{37.0}$Sn$_{110}$) DENs, and Figure 2d shows the corresponding size-distribution histogram. The average measured particle size for this bimetallic DEN is 1.3 ± 0.3 nm; however, it is not possible to calculate an accurate size for bimetallics without specific information about the packing arrangement of the atoms. TEM micrographs and size-distribution histograms for the remaining DEN compositions are provided in the Supporting Information (Figure S1). Table 1 compares the average diameters for all six G6-C$_{12}$(Ni$_x$Sn$_{(147−x)}$) DENs examined in this study. With the exception of G6-C$_{12}$(Sn$_{147}$), all of the measured diameters are lower than would be expected on the basis of the calculated sizes of the monometallics. This may be a consequence of the low atomic number of Ni and the corresponding difficulty in obtaining accurate sizes for Ni-containing DENs. Note, however, that in a previous study we reported the measured diameter of a monometallic Ni$_{147}$ DEN to be 1.2 ± 0.3 nm,[40] which is comparable to 1.1 ± 0.3 nm reported here.

EDX Analysis of Bimetallic DENs. We have previously used EDX spectroscopy to determine the composition of bimetallic DENs.[3] Likewise, EDX analyses were performed here to evaluate the composition of three different bimetallic DENs: G6-C$_{12}$(Ni$_x$Sn$_{(147−x)}$) (x = 37.0, 73.5, and 110). Figure 3 provides a typical EDX spectrum for G6-C$_{12}$(Ni$_{110}$Sn$_{37.0}$). Because of the relatively low z of Ni and Sn and the correspondingly low EDX signal, it was necessary to select an area of the TEM grid supporting ∼5 DENs for these measurements. The EDX spectrum
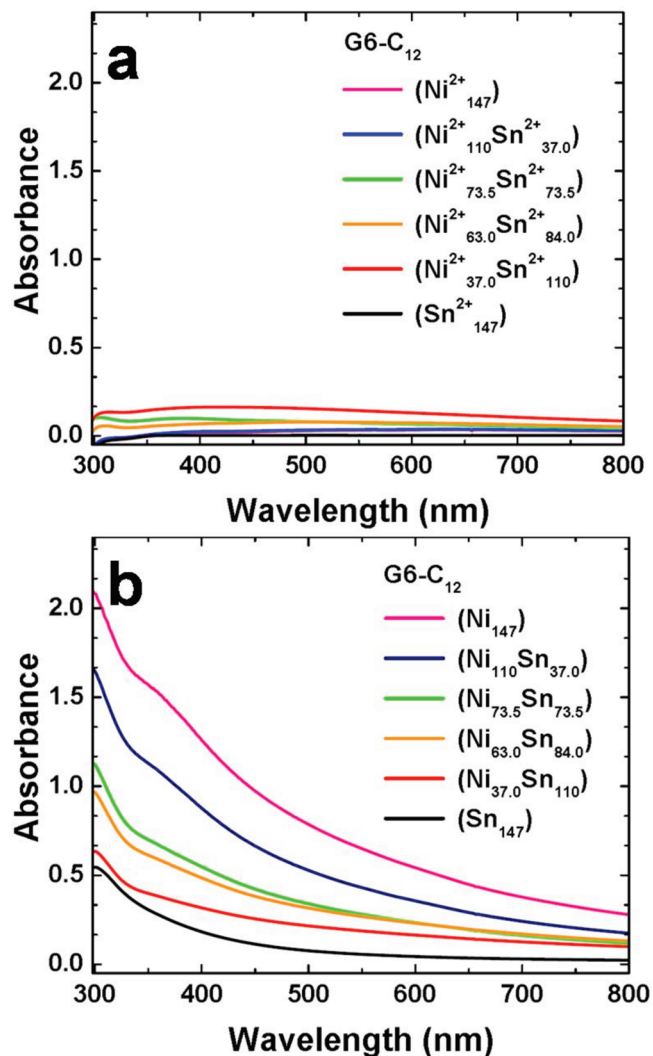

Figure 1. UV−vis absorption spectra of 2.00 μM G6-C$_{12}$-(Ni^{2+}$_x$Sn^{2+}$_{(147−x)}$) (x = 147, 110, 73.5, 63.0, 37.0, and 0) (a) before and (b) after reduction. The optical path length of the cuvette was 1.00 cm. G6-C$_{12}$ (2.0 μM) in toluene was used as the background.

reveals peaks corresponding to both the Ni (7.5 keV) and Sn (25 keV) components of the DENs. Larger peaks corresponding to the Au TEM grid were also detected in the energy range of 8−14 keV.

Quantitative atomic percentages extracted from EDX spectra such as that shown in Figure 3 are summarized in Table 2 for the three DEN compositions examined. As we have found previously for PtPd DENs,[3] the metallic compositions of G6-C$_{12}$(Ni$_x$-Sn$_{(147−x)}$) DENs closely reflect the concentrations of Ni^{2+} and Sn^{2+} used in the first step of the synthesis. We also observed that when regions of the grid that were free of visible DENs were examined by EDX, no detectable signal was observed for Ni or Sn. This is important because it implies that the values provided in Table 2 are probably reliable indicators of the composition of individual DENs even though it was necessary to examine several DENs simultaneously to obtain sufficient signal.

XPS Analysis of NiSn DENs. XPS has previously been used to determine the oxidation state of DENs.[28,31,51−57] XPS was

(50) Creighton, J. A.; Eadon, D. G. *J. Chem. Soc., Faraday Trans.* **1991**, *87*, 3881–3891.

(51) Knecht, M. R.; Weir, M. G.; Myers, V. S.; Pyrz, W. D.; Ye, H.; Petkov, V.; Buttrey, D. J.; Frenkel, A. I.; Crooks, R. M. *Chem. Mater.* **2008**, *20*, 5218–5228.
(52) Scott, R. W. J.; Ye, H.; Henriquez, R. R.; Crooks, R. M. *Chem. Mater.* **2003**, *15*, 3873–3878.
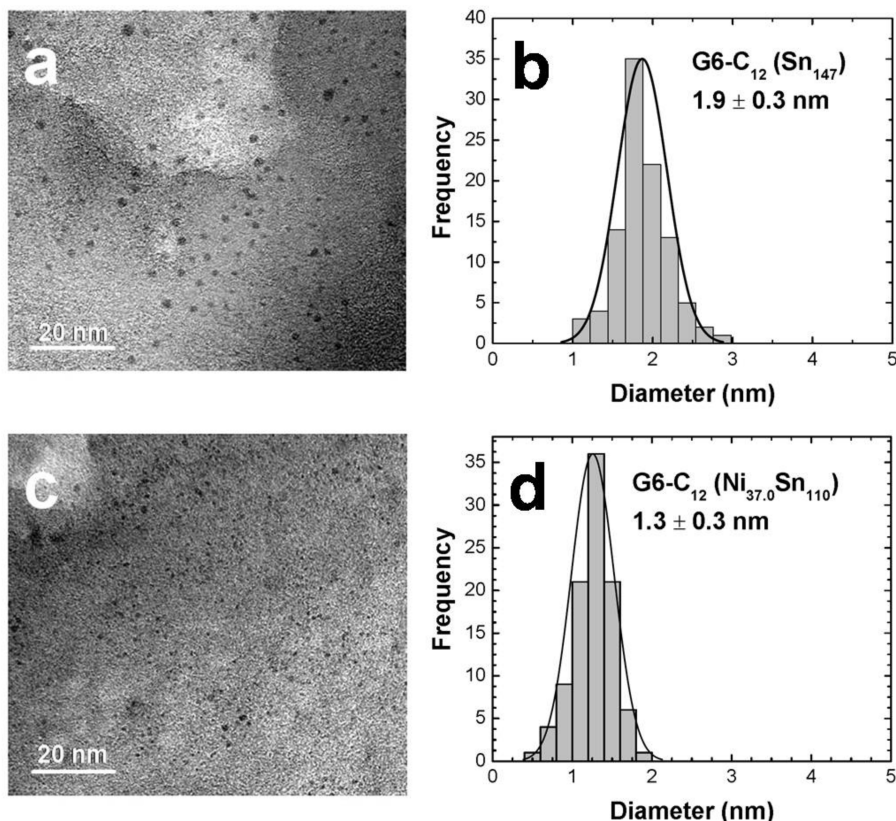
Figure 2. Bright-field TEM micrographs of (a) G6-C$_{12}$(Sn$_{147}$) and (c) G6-C$_{12}$(Ni$_{37.0}$Sn$_{110}$). The size-distribution histograms in b and d correspond to the micrographs in a and c, respectively.

Table 1. Measured and Calculated Particle Sizes for G6-C$_{12}$(Ni$_x$Sn$_{(147-x)}$) DENs

G6-C$_{12}$ DEN	average diameter (nm)	calculated value (nm)[a]
Ni$_{147}$	1.1 ± 0.3	1.45
Ni$_{110}$Sn$_{37.0}$	1.1 ± 0.2	
Ni$_{73.5}$Sn$_{73.5}$	1.2 ± 0.3	
Ni$_{63.0}$Sn$_{84.0}$	1.1 ± 0.3	
Ni$_{37.0}$Sn$_{110}$	1.3 ± 0.3	
Sn$_{147}$	1.9 ± 0.3	1.96

[a] The size calculation for monometallic nanoparticles is based on the equation $n = 4\pi r^3/3V_g$, where n is the number of metal atoms, r is the radius of the nanoparticle, and V_g is the volume of one Ni (10.9 Å^3) or Sn (27.0 Å^3) atom, derived from the molar volumes.

employed in this study to assess the oxidation state of bimetallic NiSn DENs by comparing spectra acquired before and after the reduction of the G6-C$_{12}$(Ni$^{2+}_{73.5}$Sn$^{2+}_{73.5}$) complex. The results are shown in Figure 4.

The XPS data here should be viewed with caution because of two inherent experimental limitations that may contribute uncertainty to the results. First, the dendrimers used in this study are insulating so there is a risk of surface charge accumulation during XPS measurements. For this reason, the binding-energy values
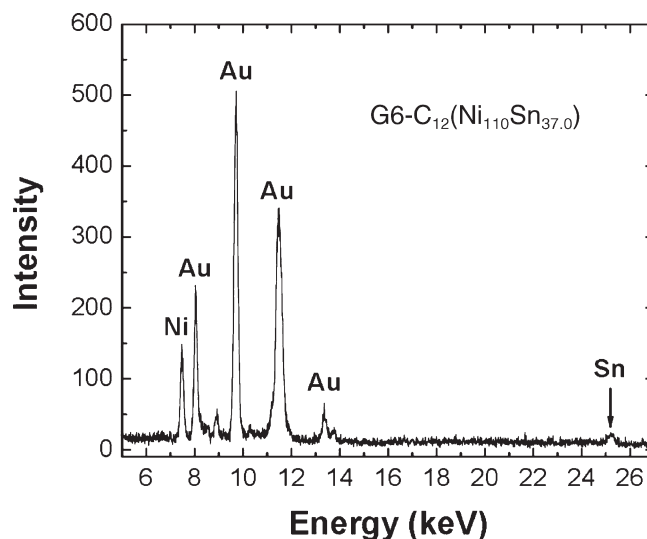

Figure 3. Representative EDX spectrum for G6-C$_{12}$(Ni$_{110}$Sn$_{37.0}$). An area on the TEM grid corresponding to about 5 DENs was used to obtain this spectrum.

are referenced to the most intense C 1s signal of the sample (285.0 eV).[59] Second, XPS detection of DENs containing metals having relatively high binding energies tends to yield poor signal-to-noise ratios. This is because the mean escape depth of, for example, Ni 2p photoelectrons is only 1 nm,[60] which is substantially less than the radius of the G6-C$_{12}$ dendrimer templates (~3 nm).

(53) Zhao, M.; Crooks, R. M. *Angew. Chem., Int. Ed.* **1999**, *38*, 364–366.
(54) Herrero, M. A.; Guerra, J.; Myers, V. S.; Gomez, M. V.; Crooks, R. M.; Prato, M. *ACS Nano* **2010**, *4*, 905–912.
(55) Ozturk, O.; Black, T. J.; Perrine, K.; Pizzolato, K.; Williams, C. T.; Parsons, F. W.; Ratliff, J. S.; Gao, J.; Murphy, C. J.; Xie, H.; Ploehn, H. J.; Chen, D. A. *Langmuir* **2005**, *21*, 3998–4006.
(56) Puniredd, S. R.; Yin, C. M.; Hooi, Y. S.; Lee, P. S.; Srinivasan, M. P. *J. Colloid Interface Sci.* **2009**, *332*, 505–510.
(57) Stofik, M.; Stryhal, Z.; Maly, J. *Bioelectronics* **2008**, *24*, 1918–1923.
(58) Moulder, J. F.; Bomben, K. D.; Sobol, P. E.; Stickle, W. F. *Handbook of X-ray Photoelectron Spectroscopy*; Physical Electronics USA, Inc.: Chigasaki, Japan, 1995.

(59) NIST X-ray Photoelectron Spectroscopy Database, version 3.5. National Institute of Standards and Technology: Gaithersburg, MD, 2003; http://srdata.nist.gov/xps/.
(60) Jin, S.; Atrens, A. *Appl. Phys. A: Mater. Sci. Process.* **1987**, *42*, 149–165.

Table 2. Percent Metallic Composition for NiSn DENs As Determined by EDX Spectroscopy

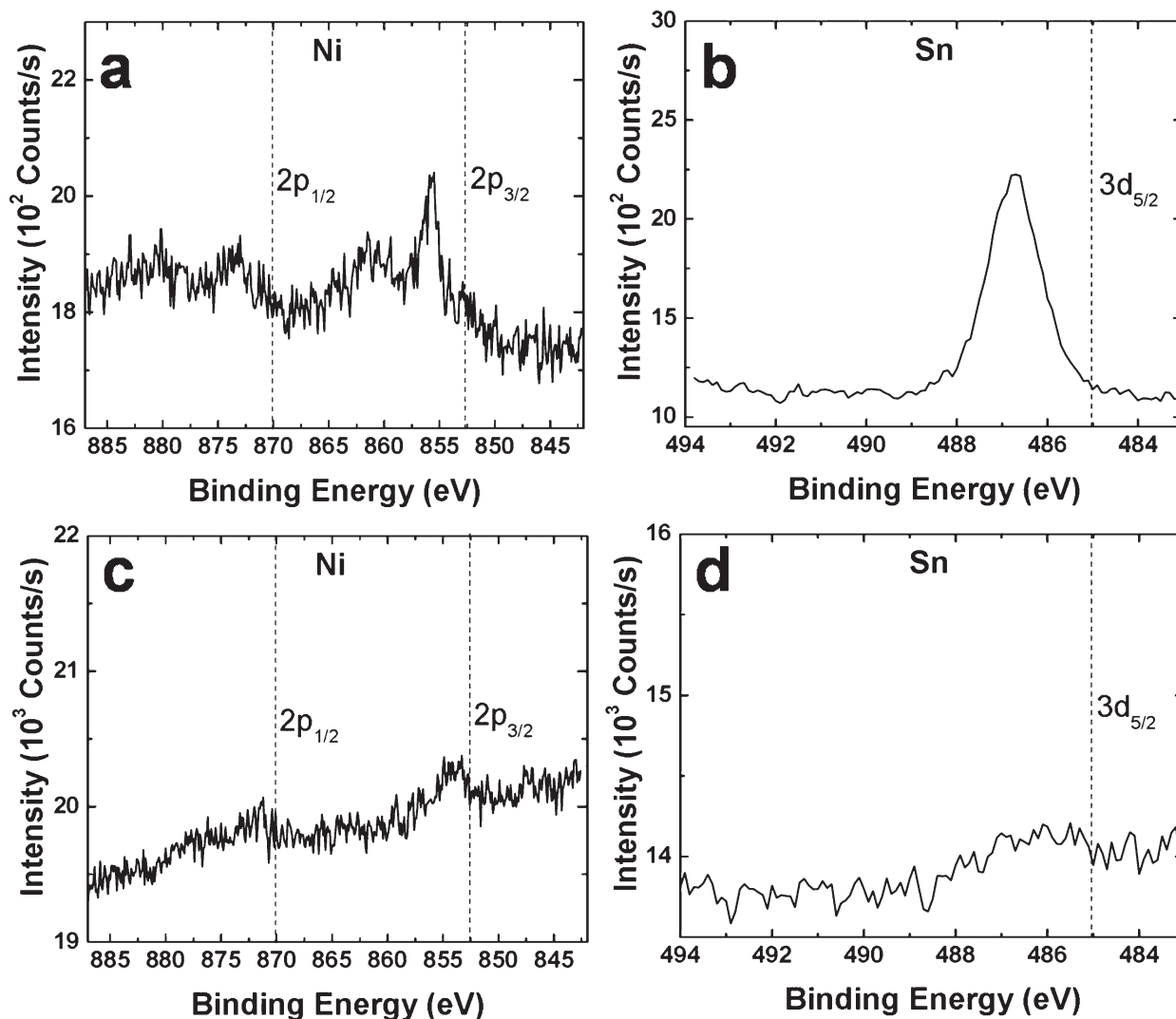| analysis no.	G6−C$_{12}$(Ni$_{37.0}$Sn$_{110}$)		G6−C$_{12}$(Ni$_{73.5}$Sn$_{73.5}$)		G6−C$_{12}$(Ni$_{110}$Sn$_{37.0}$)	
	Ni (%)	Sn (%)	Ni (%)	Sn (%)	Ni (%)	Sn (%)
1	28.7	71.3	49.6	50.4	77.2	22.8
2	28.0	72.0	50.0	50.0	76.9	23.1
3	27.1	72.9	49.9	50.1	78.3	21.7
4	27.0	73.0	49.4	50.6	75.6	24.4
5	28.6	71.4	49.7	50.3	74.8	25.2
average (SD)	27.9 (±0.8)	72.1 (±0.8)	49.7 (±0.2)	50.3 (±0.2)	76.6 (±1.4)	23.4 (±1.4)
expected	25	75	50	50	75	25

Figure 4. XPS spectra of the G6-C$_{12}$(Ni$^{2+}_{73.5}$Sn$^{2+}_{73.5}$) complex (a, b) before and (c, d) after reduction. The vertical dashed lines indicate literature values for the binding energies of the zerovalent metals.

Figure 4a,b shows high-resolution Ni and Sn XPS spectra, respectively, of the G6-C$_{12}$(Ni$^{2+}_{73.5}$Sn$^{2+}_{73.5}$) complex prior to reduction. These data were collected using the Al Kα source. Figure 4a shows a Ni 2p$_{3/2}$ peak located at 855.7 eV as well as the smaller satellite peak at 861.4 eV. The reported Ni 2p$_{3/2}$ peak position for Ni(ClO$_4$)$_2$·6H$_2$0 is 857.2 eV (obtained by two-point correction of the energy scale).[59] Figure 4b shows the corresponding XPS spectrum of the Sn^{2+} component in the bimetallic complex. The Sn 3d$_{5/2}$ peak is located at 486.8 eV. We were unable to find literature values for the binding enery of Sn(CF$_3$SO$_3$)$_2$ for comparison, but the approximate binding-energy range for Sn^{2+} 3d$_{5/2}$ is 486.0−487.5.[58] The key point is that there is nothing

notable about the Ni and Sn binding energies prior to reduction of the complex.

Figure 4c,d shows high-resolution XPS spectra of the G6-C$_{12}$(Ni$_{73.5}$Sn$_{73.5}$) DENs in the Ni and Sn regions, respectively, after the addition of the reducing agent. To increase the sample signal, these data were collected using the Mg Kα radiation source. Consequently, the peaks are broadened. Furthermore, there is greater uncertainty in charge compensation correction due to a broad C 1s signal. Further details regarding the C 1s peak are provided in the Supporting Information (Figure S2). The presence of zerovalent Ni is indicated by a weak 2p$_{3/2}$ signal at ∼854 eV, which is close to the reported binding energies for fully

reduced Ni (852.73 eV,[59] indicated by the dashed lines in Figure 4).[59] The presence of reduced Ni in the bimetallic nanoparticles is in agreement with the findings of our previous study of monometallic Ni DENs.[40] The reduction of Sn^{2+} is indicated by a weak Sn $3d_{5/2}$ signal at ~486 eV, which is shifted toward the binding energy of the zerovalent metal (484.98 eV,[59] dashed line). Although there remains some ambiguity regarding the exact oxidation state of the Sn component, because of the weak signal, the width of the peak, and the intimate presence of Ni, Sn is clearly in a significantly more reduced state than in the original complex. The relatively weak XPS signals obtained for NiSn DENs are primarily attributed to the nanoparticles being sequestered deep within the bulky G6-C_{12} dendrimers.

Finally, the NiSn DENs were exposed to air for < 2 min during transfer into the XPS instrument. We were initially surprised that these DENs did not revert back to their fully oxidized state during this exposure. However, recent experiments have shown that dendrimers tend to collapse tightly around encapsualted nanoparticles in poor solvents[16] and in gases,[61] thereby protecting them from atmospheric oxygen.

Summary and Conclusions

We have described the use of a hydrophobic dendrimer templating method to synthesize nearly monodisperse ~1.2 nm bimetallic NiSn nanoparticles in toluene. UV−vis, TEM, and EDX data support the formation of bimetallic nanoparticles having elemental compositions close to the predicted values. XPS studies reveal that the peaks corresponding to Ni and Sn in the metal ion/dendrimer complex decrease in intensity and shift to lower binding energies upon reduction, indicating the formation of DENs. However, there is some abiguity about the precise oxidation state of these materials after reduction. The results reported here are relevant to our efforts to prepare well-defined nanoscale NiSn materials for use as anodes in Li ion batteries.

Supporting Information Available: TEM micrographs and size-distribution histograms of the NiSn DEN compositions not shown in Figure 2 and high-resolution XPS spectra of the C 1s region that were used to calibrate the spectra shown in Figure 4. This material is available free of charge via the Internet at http://pubs.acs.org.

(61) Albiter, M. A.; Crooks, R. M.; Zaera, F. *J. Phys. Chem. Lett.* **2010**, *1*, 38–40.